Hindawi
Advances in Materials Science and Engineering
Volume 2019, Article ID 4065301, 12 pages
https://doi.org/10.1155/2019/4065301

Research Article

Research on Shear Capacity and Checking Method of MT·G-Joint for Application in Prefabricated Underground Structures

Xiuren Yang,[1,2,3] **Zhongheng Shi**,[1] **and Fang Lin**[2,3]

[1]*School of Civil Engineering, Beijing Jiaotong University, Beijing 100044, China*
[2]*Beijing Urban Construction Design and Development Group Co. Ltd., Beijing 100037, China*
[3]*National Engineering Laboratory for Green & Safe Construction Technology in Urban Rail Transit, Beijing 100037, China*

Correspondence should be addressed to Xiuren Yang; yangxr@bjucd.com and Fang Lin; felyo@foxmail.com

Received 2 August 2019; Revised 11 October 2019; Accepted 30 October 2019; Published 12 November 2019

Academic Editor: Yee-wen Yen

The MT·G-Joint (grouted mortise-tenon joint), invented as the connection between the large prefabricated elements, is the most important component in the prefabricated underground structures. Its shear performance is critical to the overall mechanical performance of the prefabricated structure. This paper carries out four-point pure shear experiment to investigate the shear performance of the MT·G-Joint. The shear key method is then proved to be suitable for MT·G-Joint when the axial load is 0 kN based on the experimental results. In addition, combining the shear key method and experimental results, the calculation method of the shear capacity, improved shear key method (ISKM), is proposed on account of the mechanical model of the failure plane. ISKM is appropriate for different load conditions. Finally, every kind of joints used in the prefabricated metro station structures on Changchun Metro Line 2 is calculated by using ISKM. The results indicate that the shear capacity of the MT·G-Joint is good, and the used joints still have large safety margin even under the worst working condition. The findings of this study are of value to help researchers and engineers more effectively design prefabricated underground structures.

1. Introduction

With the rapid development of rail transit construction in China, social environmental awareness increases continuously. Moreover, long and tight construction period, large resource consumption, shortage of skilled labour, and not guaranteed structure quality bring great challenges to traditional construction technology of metro station. Above situations are particularly prominent in the northeast of China. Like Changchun city, located in the northeast region, is so cold that 4~5 months' winter break is needed for metro construction. All these issues cause huge deadline pressure and make it hard to guarantee construction quality under low temperature. To solve these problems and promote sustainable urban development, prefabricated technology of the underground structure was first researched and developed in China since 2012 to reduce resources consumption, overcome winter construction problems in cold region. Up to the present, five metro stations using this technology have been built on Changchun Metro Line 2 [1, 2].

The five cut-and-cover stations are all supported by anchor-pile system, and all those horseshoe-shaped two-storey stations are 20.5 m wide and 17.45 m high. The full prefabricated station structure is built by assembling seven 2 m wide prefabricated components without any concrete wet spraying (see Figure 1). The MT·G-Joint (grouted mortise-tenon joint) is developed and used for connecting adjacent prefabricated components (see Figure 2, Chinese patent number: ZL201420165101.X).

For prefabricated technology used in underground engineering, prefabricated linings were firstly applied in the shield tunnel with a circular section in the late 19th and early 20th century [3, 4]. For other kinds of underground structures, prefabricated technology was used in underground engineering in Netherlands, France, and Japan [5]. However, limited to the technological conditions at that

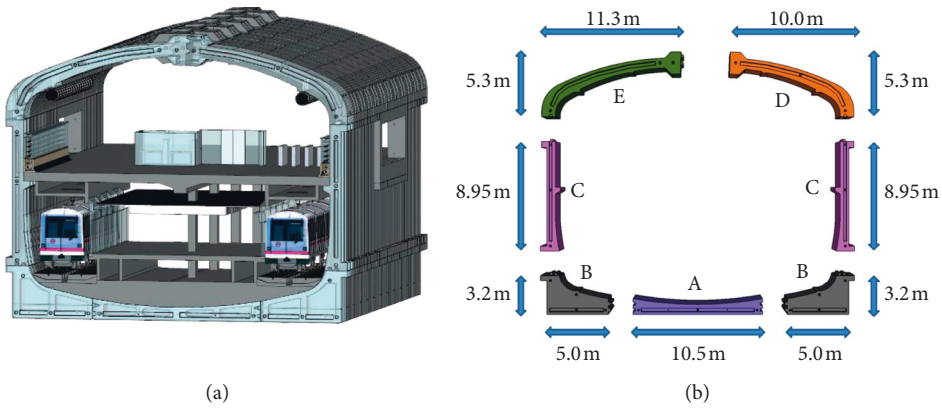

Figure 1: Prefabricated metro station.

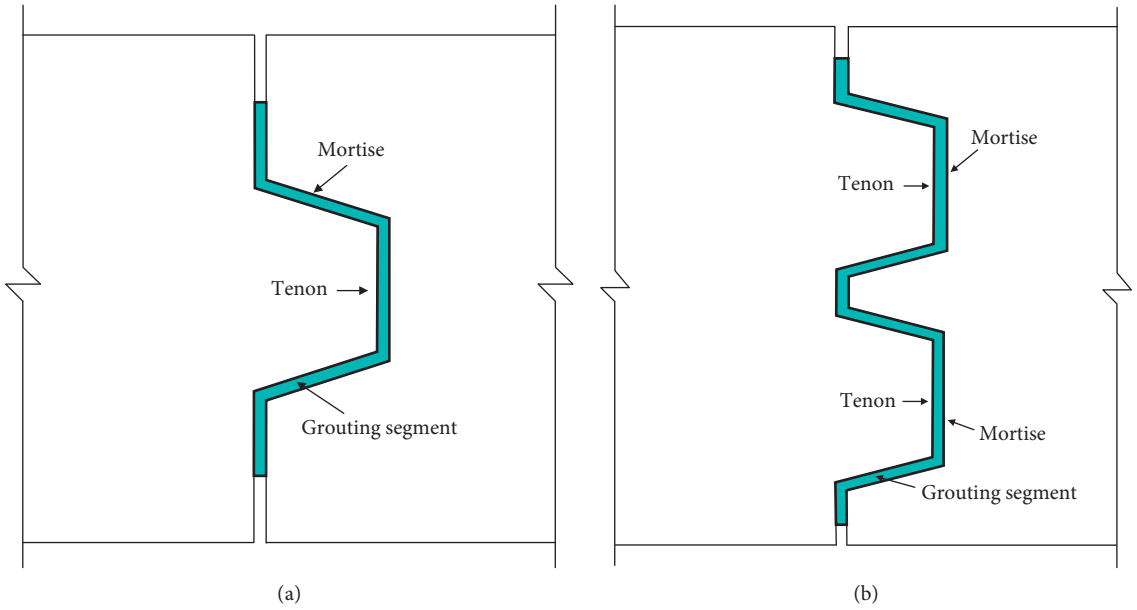

Figure 2: The MT·G-Joint used on Changchun Metro Line 2. (a) Single tenon. (b) Double tenon.

time, connection joints used cast-in-place concrete, which have difficulty in waterproofing. Up to now, the prefabricated technology is more for use in simple structure with small cross-section like metro running tunnel and municipal pipeline [6–8]. Moreover, research on prefabricated technology of large underground structure, especially on full prefabricated technology, is rare.

Joint is critical to the overall mechanical performance of the prefabricated structure, especially the shear performance. MT·G-Joint consists of mortise, tenon, and grouting segment filled with improved epoxy resin, and all of these elements work together to carry shear force, which leads to the complexity of mechanism. Therefore, it is necessary to carry on in-depth research on the shear behaviour of the MT·G-Joint.

Mortise and tenon of the joint working together transfer the shear effect as shear key, and Japanese researchers have developed the clear calculation method of the shear key [9]. It is demonstrated that the shear capacity of the joint is the smaller value between the shear strength of the joint and concrete compressive strength of the mortise and tenon.

As shown in Figure 3, shear strength of the shear key Q_{sk} is the smaller value between the strength of left shear key Q_1 and the strength of right shear key Q_2:

$$Q_{sk} = \min(Q_1, Q_2), \tag{1}$$

$$Q_1 = \min(Q_{1s}, Q_{1b}), \tag{2}$$

$$Q_2 = \min(Q_{2s}, Q_{2b}), \tag{3}$$

$$Q_{1b} = \alpha \cdot f'_{c1} \sum_{i=1}^{n} (w_i \cdot x_i), \tag{4}$$

$$Q_{2b} = \alpha \cdot f'_{c2} \sum_{i=1}^{n} (w_i \cdot x_i), \tag{5}$$

$$Q_{1s} = 0.5 \cdot \sqrt{f'_{c1}} \sum_{i=1}^{n} (a_i \cdot w_i), \tag{6}$$

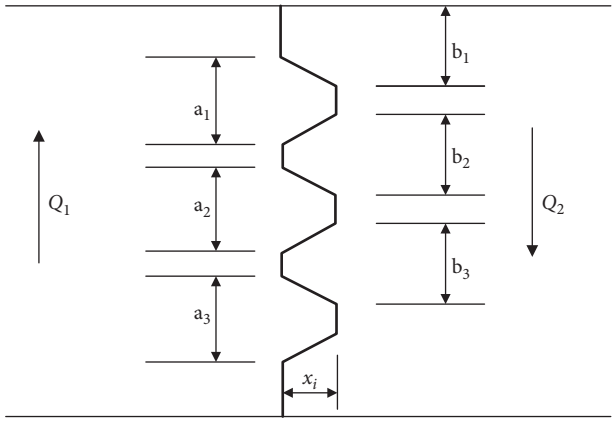

Figure 3: Shear bearing of mortise and tenon joints.

$$Q_{2s} = 0.5 \cdot \sqrt{f'_{c2}} \sum_{i=1}^{n} (b_i \cdot w_i), \quad (7)$$

where Q_{1s} and Q_{2s} are the shear strengths of the joint generated from the left and right interfaces, respectively; Q_{1b} and Q_{2b} are the concrete compressive strengths of the left and right interfaces, respectively; n denotes the number of shear key bearing stress; w_i is the width of shear key; x_i is the height of shear key; f'_{c1} denotes concrete compressive strength of left interface (N/mm^2); f'_{c2} denotes concrete compressive strength of right interface (N/mm^2); α is the bearing coefficient, which is 1.0 [9]; and a_i and b_i are the bottom lengths of shear key.

Using the above shear key method, the shear capacities of the joints used in the prefabricated metro station are calculated with equations (1)–(7): 825.35 kN for single-tenon joint and 1593.78 kN for double-tenon joint per meter (see Figure 4).

However, as we know from previous studies [1, 2], the load-carrying behaviour of the MT·G-Joint varies with load condition based on extensive joints experiments. It means the shear capacities are not constant values as the above calculation. In addition, shear key method is suitable for the joint with unbroken key and small deformation [9]. Furthermore, the MT·G-Joint consists of not only mortise and tenon but also grouting segment in the interface between mortise and tenon. Therefore, the shear experiment is conducted to further investigate the more precise calculation method of shear capacity for the MT·G-Joint.

2. Experimental Design

Figures 5 and 6 display the layout of four-point pure shear experiment. Single-tenon specimen is 1 : 1 prototype in key working direction (the cross-sectional direction in Figure 1), and the width reduces from 2000 mm to 800 mm in nonkey working direction (longitudinal direction). The specimen is lying in the experimental pit with axial force 0 kN in the both ends. One jack applies a vertical load to induce shear force via a load distribution girder. The shear force is applied using displacement control at a rate of mm. Two supports are antisymmetric to the loading points in the other side of the specimen. The region between the left support and the right loading point including the tenon and mortise is the pure-shear part. Figure 7 demonstrates the test elements—steel and concrete strain gauges and displacement meters.

3. Experimental Results and Discussion

3.1. Law of Cracks Development. When the shear force is 356 kN, the initial crack begins from the bottom of the mortise close to the loading side and develops along the bottom side of the mortise of 60° (see Figure 8). At the last moment, one through crack begins from the left loading point and develops along the bottom side of the specimen of 45°. In addition, the grouting segment does not break away from the concrete surface within the whole loading period.

3.2. Law of Stress Development. Figure 9 presents the change curves of concrete stress in the (a) outer region of the mortise and tenon and (b) inner region of the mortise and tenon. The first inflection point turns up when the shear force comes to 350 kN (83#, 84#, and 85# in (a) and 60# in (b)), which is close to the value of crack appearance. Subsequently, the compressive stress of 71# in the wall of the tenon and 67# in the foot of the tenon increase significantly in the later loading period. At last, 83#, 84#, and 103# come to the compressive stress limit state. In addition, most gauging points are in tension and the tensile stress increases to the limit state with loading. It also shows that the most active region of the curve is the four corners of the mortise and tenon, which means the occlusion between the mortise and tenon plays a key role in shear resistance.

Figure 10 illustrates the change curves of steel stress with loading using the same regional division ((a) and (b)) as concrete stress. As we can see from Figure 10(b), the most active regions are the four corners and the walls of the mortise and tenon like 28#, 4#, 8#, and 31#. Especially, the two top corners of the tenon show the tensile state at the beginning and keep increasing to yielding. 30# in Figure 10(a), located in the force acting point, stays unchanged since loading begins but yields suddenly at 360 kN. The value is close to crack appearance. The other gauging points are in tensile state with a little change.

3.3. Shear Performance. Relationship of shear force Q and deflection δ is derived in Figure 11. It can be seen that there are two obvious inflection points from the curve. One is 430 kN; after that, the curve drives into nonlinear segment from the almost linear segment. The other is 570 kN; after that, the slope of the curve goes to an apparent decline. The contour map of the concrete stress development is plotted in Figure 12 based on the experiment results of concrete stress with using Surfer 12. Figure 12 illustrates four states: (a) crack appearance, (b) inflection point①, (c) inflection point②, and (d) utmost load. It is found that the compressive stress concentration happens in the waist of the mortise and tenon. This phenomenon has only been found in the bottom side when crack appears. It also appears in the top side, and the range expands with loading. At the ultimate

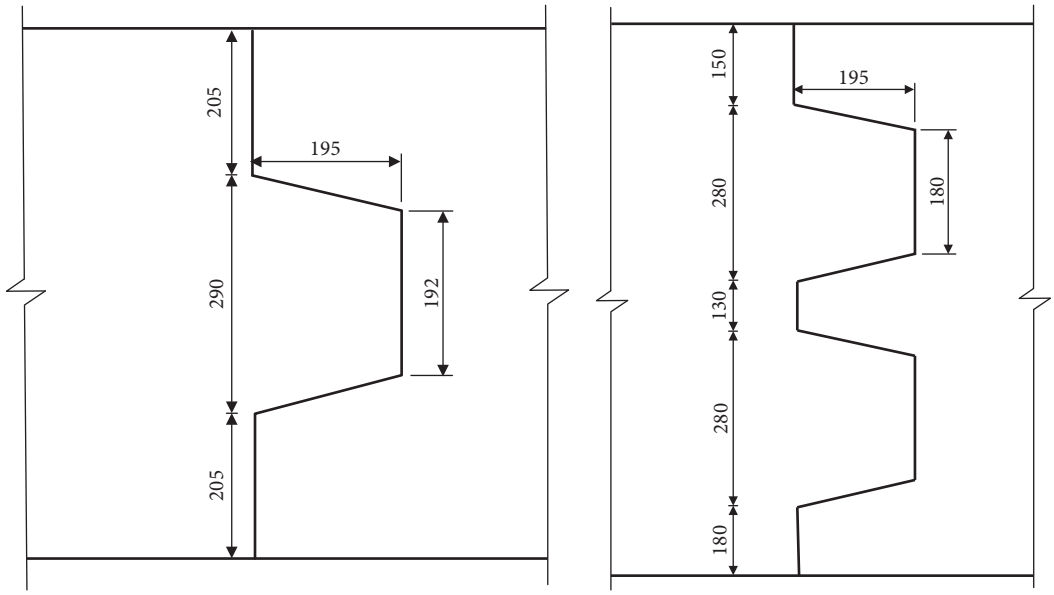

Figure 4: The joint size of (a) single-tenon and (b) double-tenon.

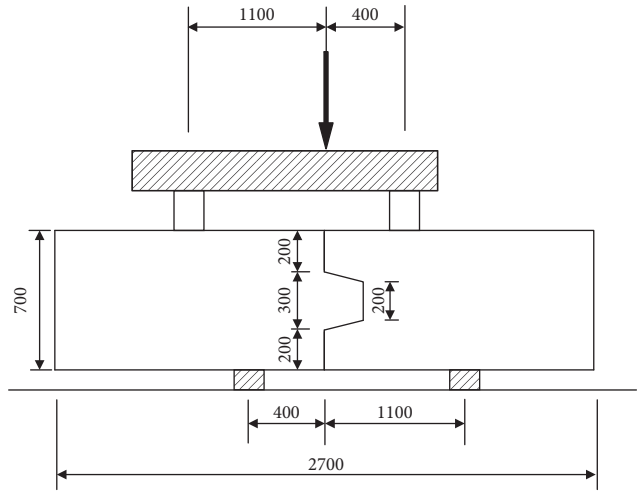

Figure 5: Sketch map of the four-point shear experiment.

carrying moment, the compressive stress concentrates in the both sides of the mortise and tenon's waist and the foot of the tenon in the top side. In addition, compressive stress limit occurs in the bottom side of the mortise and tenon's waist. The other regions stay in tension at this moment. In brief, stress concentration in the region of the mortise and tenon demonstrates the occlusion relationship of the mortise and tenon has a significant effect on the joint's performance.

Furthermore, secant stiffness (red line) as $4.16{\cdot}10^5$ kN/m and equivalent stiffness of the complete period (blue line) as $6.93{\cdot}10^4$ kN/m are derived from Figure 11. In addition, the shear capacity is obtained as 668 kN, which is approximately equal to the calculated value 660.28 kN in shear key method. Therefore, it is clear that the grouting segment in the seam restricts the deformation of the mortise and tenon, which keeps the completeness of the shear key and guarantees the carrying capacity of the joint. It can also be demonstrated that the shear key method is suitable for the MT·G-Joint when the axial load is 0 kN. Next, the calculation method of the shear capacity under different load conditions is further studied in the following section.

4. Calculation Method of Shear Capacity

4.1. Shear Resistance Analysis of Mortise and Tenon Joints. As we know from the experiments, the root cause of the crack is that the concrete tensile stress reaches the ultimate tensile strength f_t. The vertical shear stress τ, tensile stress f_t, and normal stress σ_n have below relations as shown in Figure 13, when the joint is broken along the root of the tenon or main crack.

The angle between principal tensile stress and horizontal direction is about 37° from the experimental results. The

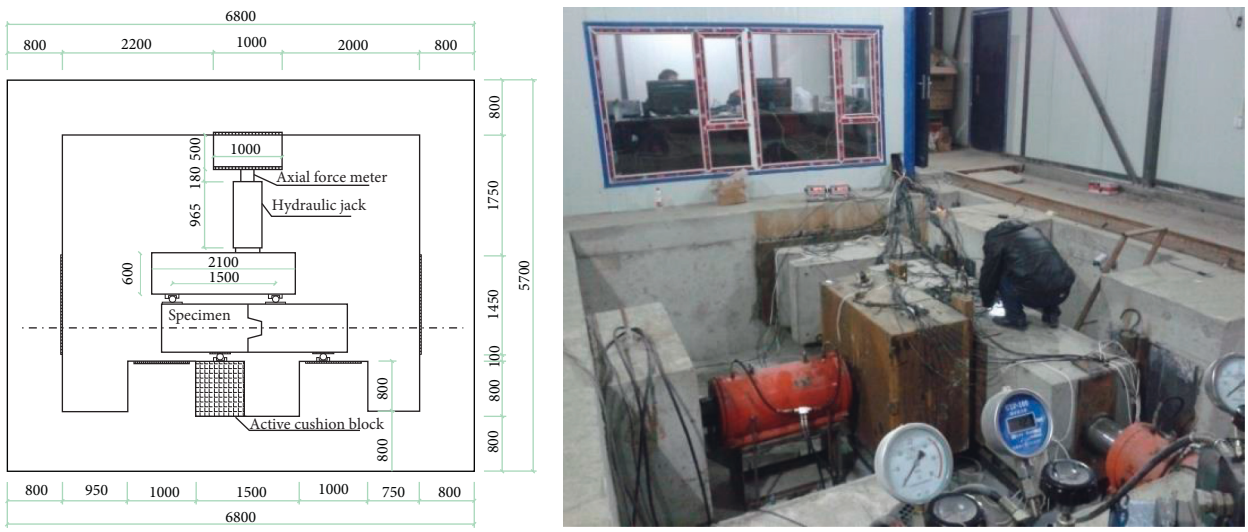

Figure 6: Layout of the experimental loading system.

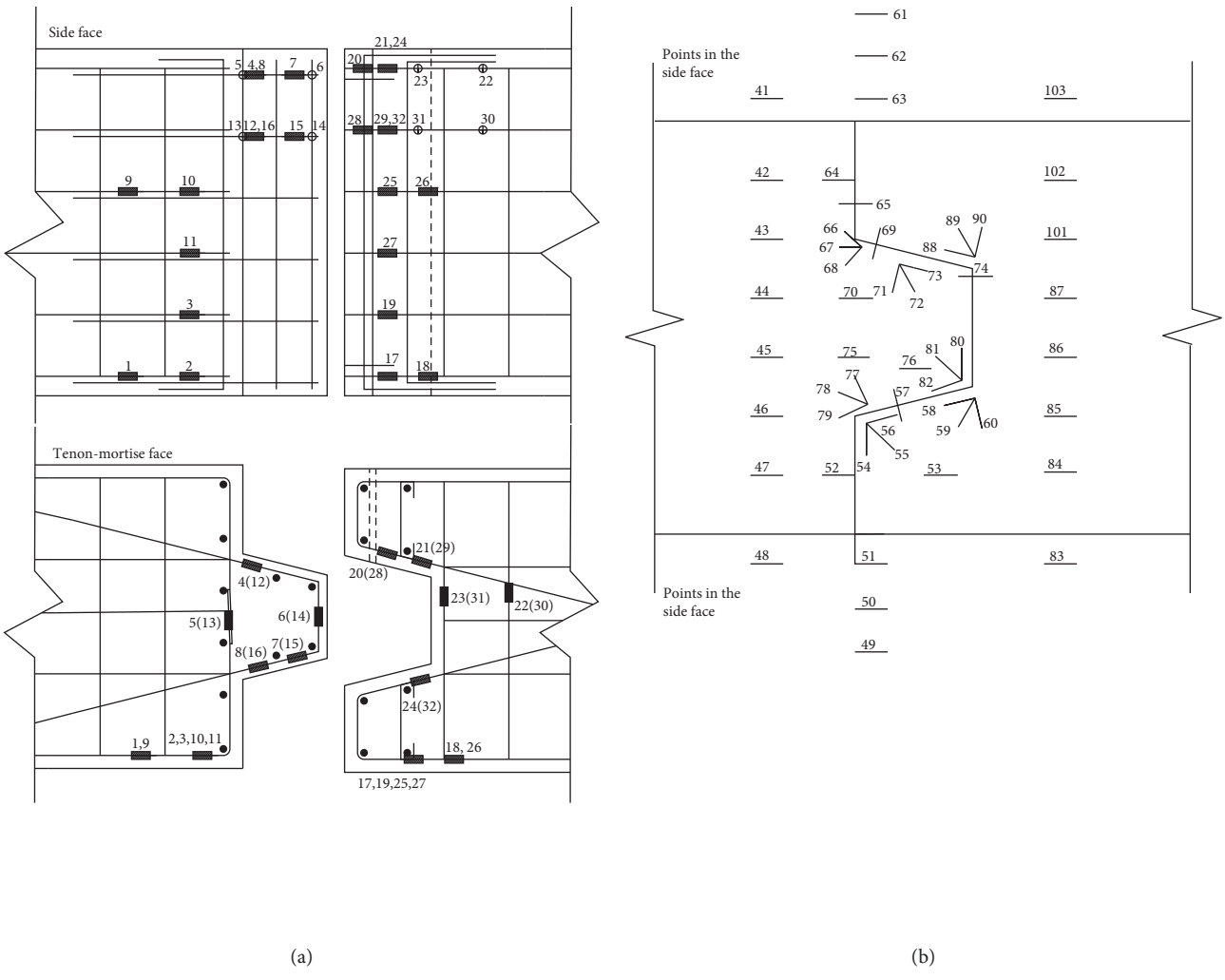

Figure 7: Continued.

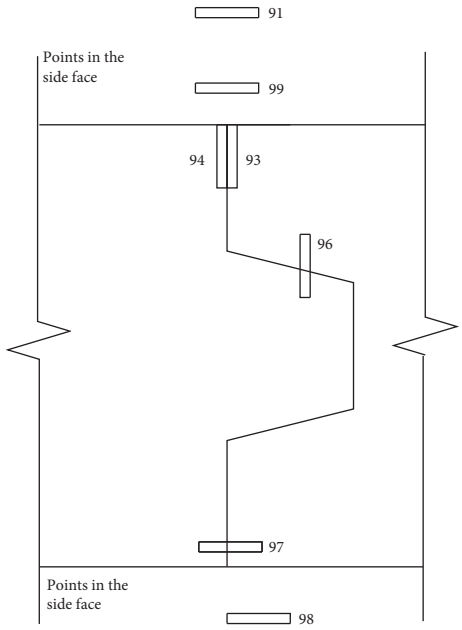

(c)

(d)

(e)

(f)

Figure 7: Test elements. (a) Steel strain gauges layout. (b) Concrete strain gauges layout. (c) Displacement meters layout. (d) Arrangement of steel strain gauges. (e) Arrangement of concrete strain gauges. (f) Arrangement of displacement meters.

principal tensile stress arrives at f_t when the joint comes to the ultimate state. Figure 14 displays Mohr's circle of the microunit in the failure plane of the mortise and tenon joint at this moment. According to the equilibrium relationship and stress relationship in the microunit, the following equations are obtained:

$$\begin{aligned} \frac{\tau_x}{\sin 2\alpha} &= \frac{\tau_x}{\tan 2\alpha} + \sigma_x + f_t, \\ \tau_x &= \tau_y = \tau, \\ \sigma_x &= \sigma_n. \end{aligned} \tag{8}$$

The concrete vertical shear stress τ of the mortise and tenon when broken can be solved from the above simultaneous equations:

$$\tau = \frac{\sin 2\alpha}{1 - \cos 2\alpha}\left(f_t + \sigma_n\right) = 1.327\left(f_t + \sigma_n\right). \tag{9}$$

Furthermore, the concrete axial tension strength f_t and the axial compressive strength f_{cu} have the following empirical relation [10]:

$$f_t = 0.26 f_{cu}^{2/3}. \tag{10}$$

Consequently,

$$\tau = 0.345 f_{cu}^{2/3} + 1.327\sigma_n. \tag{11}$$

4.2. Calculation Method. Based on the shear experimental results in this study and other shear experimental researches on cemented key-tooth for the prefabricated bridge beam segment [11–20], it is demonstrated that the baroclinic cracks are fully developed, and the main slab crack is formed in the key-tooth when the joint is submitted to the shear failure. In addition, the grouting segment does not break away from the concrete surface in this study, which means the joint has good overall performance. Therefore, the failure surface of the MT·G-Joint can be regarded as the whole concrete interface, and the calculation formula of this joint can be described as

$$Q_{sk} = \alpha_s \tau A_s = \alpha_s A_s\left(0.345 f_{cu}^{2/3} + 1.327\sigma_n\right), \tag{12}$$

where A_s is the total area of the failure plane, which is the area of the tenon's root in simplify here, mm^2; α_S is

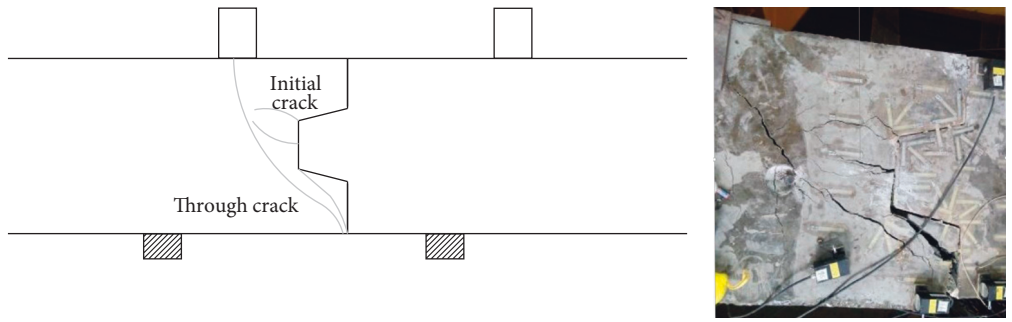

Figure 8: Final failure mode.

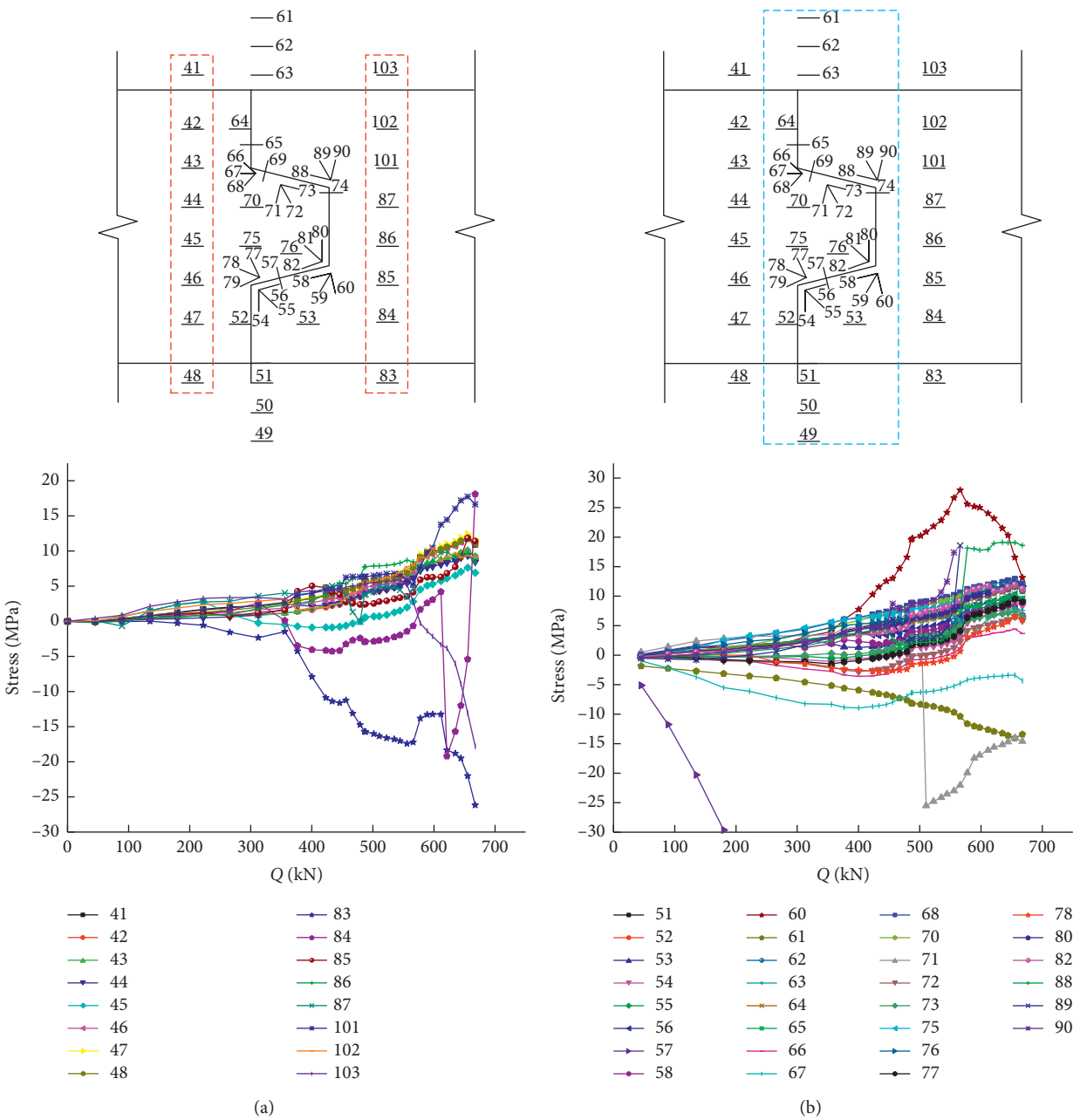

Figure 9: Change curve of concrete stress with bending moment.

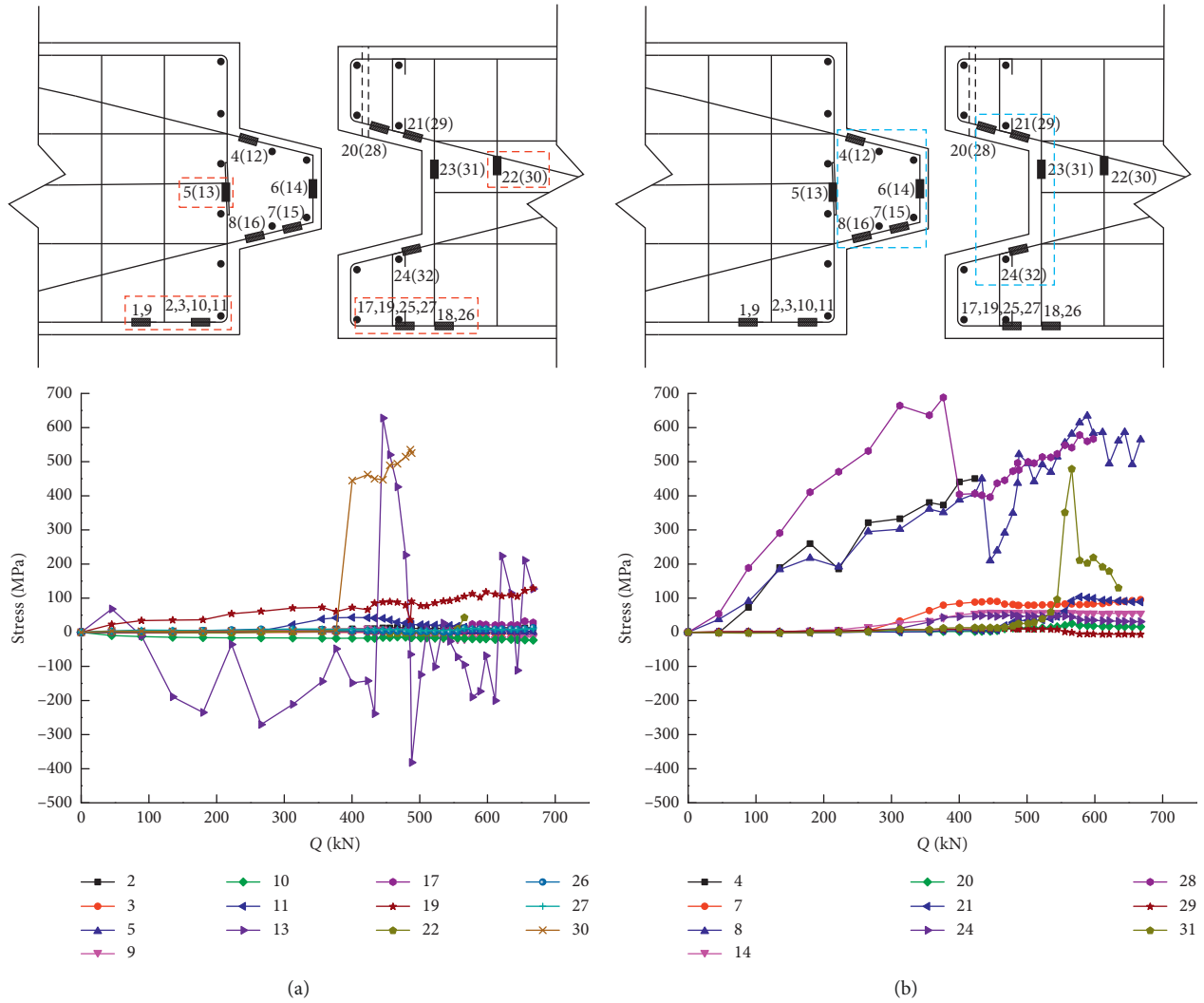

Figure 10: Change curve of steel stress with bending moment.

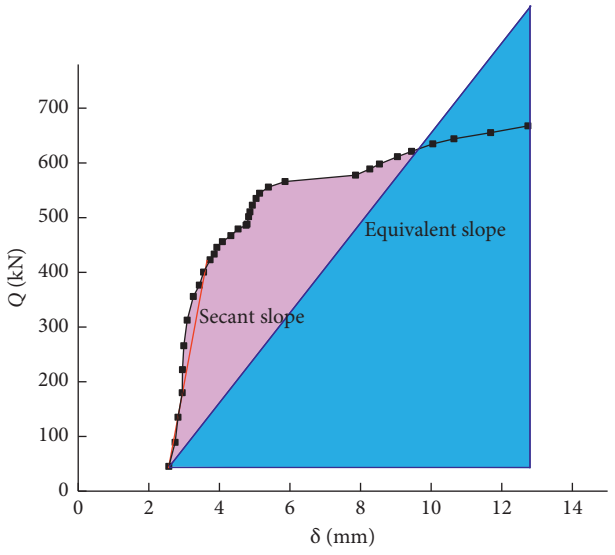

Figure 11: Relation curve of Q-δ.

introduced as reduction coefficient for the grouting seam, according to the pure shear experiment ($N = 0$, $\sigma_n = 0$), $\alpha_S = 0.81$ is calculated as the suggested value; σ_n denotes the normal stress of the interface, $\sigma_n = N/bh$, MPa; b is the width; and h is the contact height of the joint, when a pretightening rod is applied in the joint, $\sigma_n = (N + T)/bh$; and T is the pretightening force, as shown in Figure 15.

When $N = 0$, $\sigma_n = 0$, Q_{sk} can be calculated in the above equation (12): $Q_{sk} = 0.345\alpha_s A_s f_{cu}^{2/3} = 659$ kN. This calculated value is approximately equal to the calculated value (660 kN) using the shear key method and experimental result (668 kN). Therefore, both calculation methods are workable when $N = 0$. On the one hand, the underground structure is surrounded by the soils ($\sigma_n \neq 0$), which is not considered in the shear key method. On the other hand, the shear key method is mature and widely used in the prefabricated structure. In addition, there is no difference if it is cemented or dry connection when using the shear key method. Moreover, the geometrical size of the mortise and tenon joint can be taken into account.

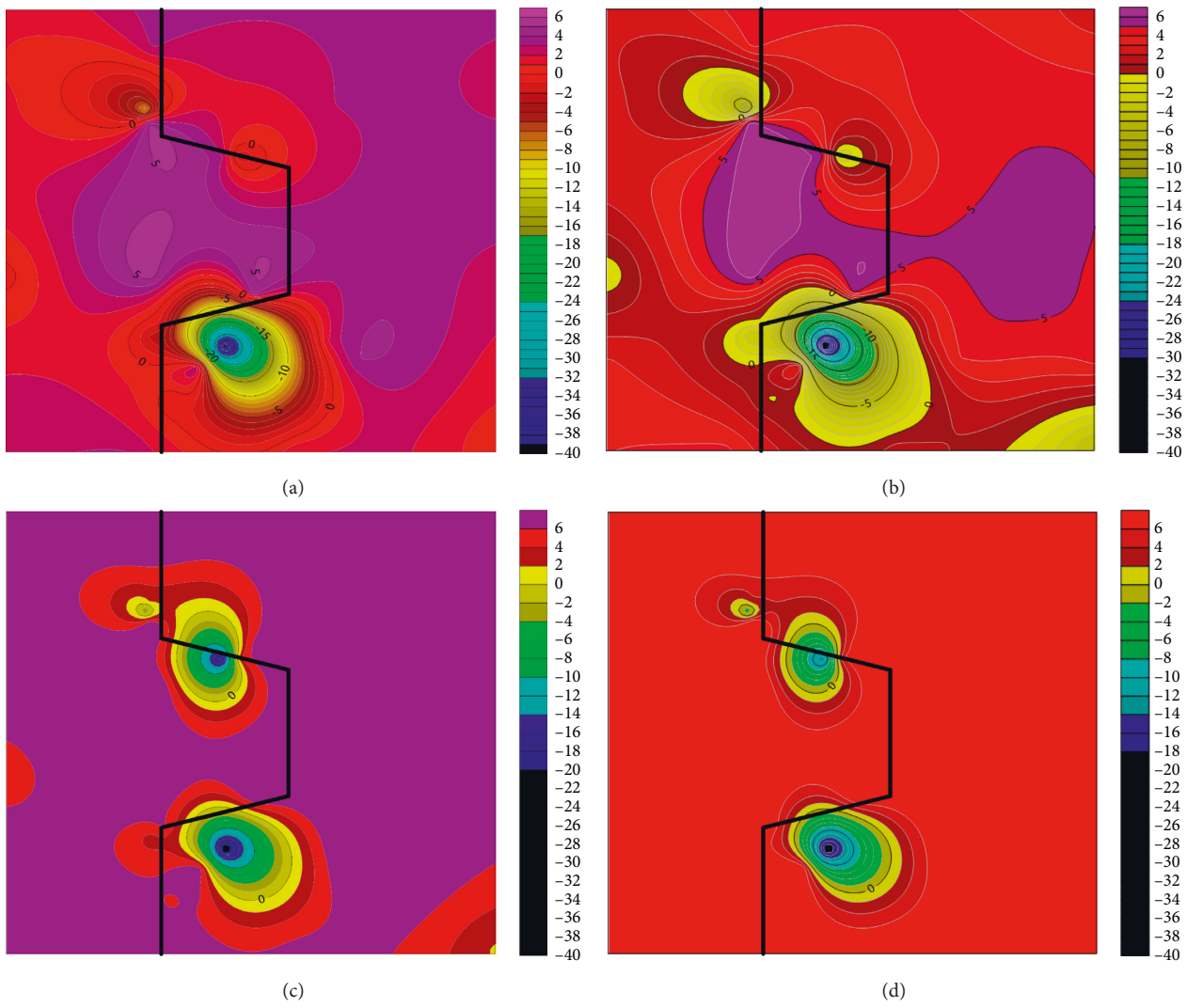

Figure 12: Contour map of concrete stress development. (a) Crack appearance. (b) Inflection point①. (c) Inflection point②. (d) Utmost load.

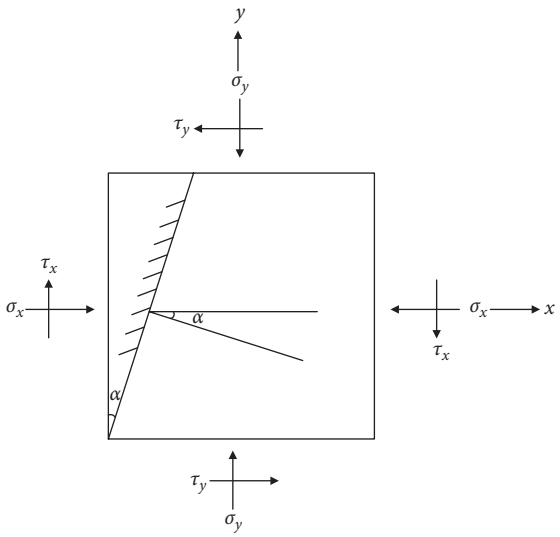

Figure 13: Microunit plane stress state in the failure plane of the mortise and tenon joint.

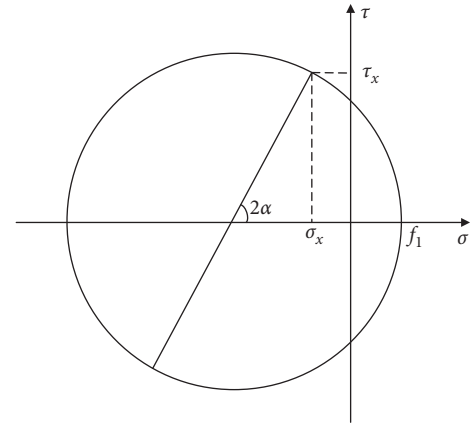

Figure 14: Mohr's circle of microunit.

Therefore, based on the shear key method, this study replaces the parts without axial force in equation (12) with the shear key method and divides A_s of the parts with axial force into the

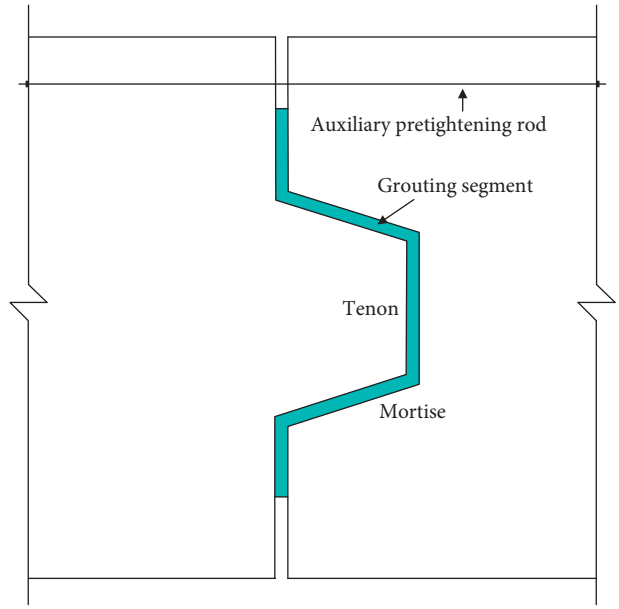

Figure 15: MT·G-Joint with an auxiliary pretightening rod.

tenon part $\sum_{i=1}^{n}(a_i \cdot w_i)$ and mortise part $\sum_{i=1}^{n}(b_i \cdot w_i)$. Finally, the reasonable calculation method—improved shear key method (ISKM)—is proposed in the following:

$$Q_{sk} = \min(Q_1, Q_2), \tag{13}$$

where Q_1 is the shear capacity of the left key and Q_2 is the shear capacity of the right key:

$$\begin{aligned} Q_1 &= \min(Q_{1s}, Q_{1b}) + Q_{1N}, \\ Q_2 &= \min(Q_{2s}, Q_{2b}) + Q_{2N}, \\ Q_{1N} &= 0.81 \cdot 1.327\sigma_n \cdot \sum_{i=1}^{n}(a_i \cdot w_i), \\ Q_{2N} &= 0.81 \cdot 1.327\sigma_n \cdot \sum_{i=1}^{n}(b_i \cdot w_i), \end{aligned} \tag{14}$$

Q_{1s}, Q_{1b}, Q_{2s}, and Q_{2b} are calculated as equations (4)~(7), respectively.

4.3. Checking Calculation. Envelope curves of the shear capacity for every kind of joints (width is 2 m) used in prefabricated metro station structures are calculated in ISKM, as presented in Figure 16. Here, the ultimate limit state (ULS) uses $f_c = 32.4\ \mathrm{N/mm^2}$, and the serviceability limit state (SLS) uses $f_c = 23.1\ \mathrm{N/mm^2}$ (C50 concrete as practical engineering). Furthermore, the shear force of every kind of joints in different working conditions under static and seismic force [21] for quasi-permanent combination and fundamental combination is calculated with the finite element method for checking in Figure 16.

It can also be clear that all the calculated values in the field are far below the ULS envelope curves. In addition, the calculated values of joint BC and CD/E are larger than the other joints. It is found that these larger values are calculated under seismic condition.

5. Conclusion

This paper conducts shear experiment to investigate the shear performance of the MT·G-Joint used in prefabricated underground structures, and based on the experimental results, the shear capacity calculation method is developed then. In addition, checking calculation of all kinds of joints used in the completed prefabricated metro station is performed. From the findings, the following consequences can be extracted:

(a) It can be seen from the four-point shear experimental results, the grouting segment in the seam does not break away from the concrete interface when broken, and the occlusion relationship between the mortise and tenon plays a significant role in shear resistance. Moreover, shear capacity of the joint under pure shear loading conditions is derived. It also verifies the practicability of the shear key method for the joints' calculation when the axial force is zero.

(b) Grouting segment, filled with the material of lower elastic modulus than the concrete between the mortise and tenon, is beneficial to the safety of the joint under loading. It also restricts the displacement and deformation of the mortise and tenon and keeps the completeness of the joint. In addition, it ensures the integrity and carrying capacity of the shear key.

(c) Through shear resistance analysis of the MT·G-Joint, the failure mode of the shear key is regarded as the shear failure of the whole concrete interface. Based on the shear key theory, combining with the experimental results and plane stress relations in the failure plane, the improved shear key method (ISKM) is proposed, which can take surrounding

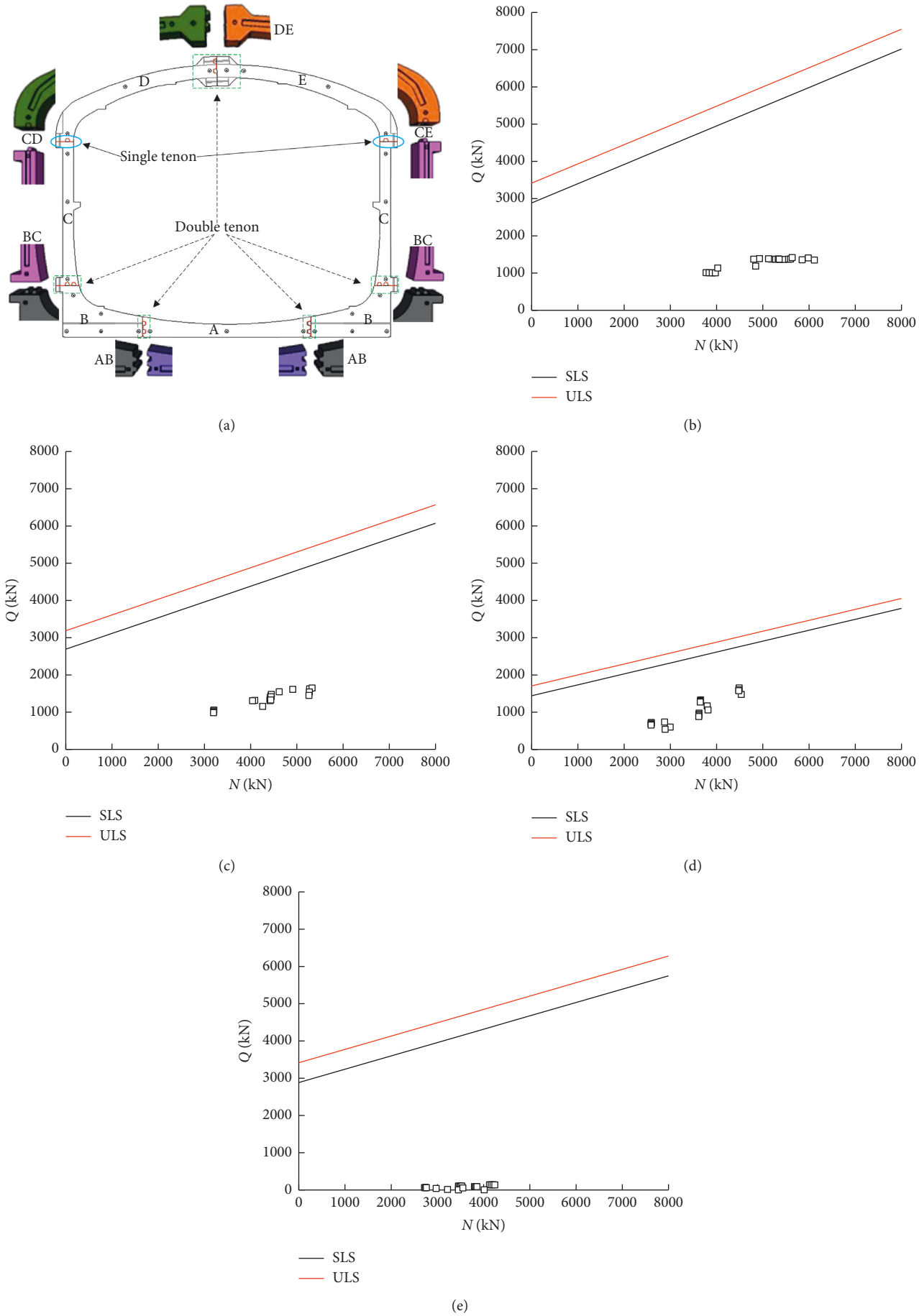

Figure 16: Checking calculation of shear capacity. (a) Distribution of all kinds of joint. (b) AB. (c). BC. (d) CD/E. (e) DE.

applied axial force and the auxiliary pretightening rod into account.

(d) Envelope curves of shear capacity for every kind of joints used in the prefabricated metro station are calculated in ISKM. Checking calculation of the shear capacity for each joint in different load conditions is also performed. It is demonstrated that the shear capacity of the joint is good and even the maximum values of different conditions still have a lot of margins to ULS.

Data Availability

The data used to support the findings of this study are available from the corresponding author upon request.

Conflicts of Interest

The authors declare that they have no conflicts of interest.

Authors' Contributions

Xiuren Yang supervised the project and developed the concept and methodologies with Zhongheng Shi. Fang Lin performed the experimental and theoretical studies.

Acknowledgments

This research was funded by the National Key S&T Special Projects (grant no. 2017YFB1201104).

References

[1] X. R. Yang, M. Q. Huang, and F. Lin, "Research strategies on new prefabricated technology for underground metro stations," *Urban Rail Transit*, vol. 5, no. 3, pp. 145–154, 2019.

[2] X. R. Yang, Z. H. Shi, and F. Lin, "Influence of geometrical parameters on performance of grouted mortise and tenon joints for application in prefabricated underground structures," *Advances in Civil Engineering*, vol. 2019, Article ID 3747982, 14 pages, 2019.

[3] L. Rozsa, "Precast concrete segment lining of the Budapest Metro," *Tunnels & Tunnelling International*, vol. 11, no. 10, 1979.

[4] J. H. Liu and X. Y. Hou, *The History of Shield Tunneling*, China Railway Press, Beijing, China, 1991.

[5] K. B. Beilasov, Q. H. Qian, and C. Z. Qi, *The Essence of the Construction of Russian Underground Railway*, China Railway Press, Beijing, China, 2012.

[6] S. Teachavorasinskun and T. Chub-Uppakarn, "Influence of segmental joints on tunnel lining," *Tunneling and Underground Space Technology*, vol. 25, no. 4, pp. 490–494, 2010.

[7] D. A. Steinhardt and K. Manley, "Adoption of prefabricated housing-the role of country context," *Sustainable Cities and Society*, vol. 22, pp. 126–135, 2016.

[8] B. Tvede-Jensen, M. Faurschou, and T. Kasper, "A modelling approach for joint rotations of segmental concrete tunnel linings," *Tunnelling and Underground Space Technology*, vol. 67, pp. 61–67, 2017.

[9] Japanese Prefabricated Building Association, *Pandect of Prefabricated Buildings*, China Architecture & Building Press, Beijing, China, 2012.

[10] Z. H. Guo, *Strength and Deformation of Concrete*, Tsinghua University Press, Beijing, China, 1997.

[11] S. T. Song, "Experimental study and theoretical analysis in bending and joint shear of high-speed railway precast segmental concrete box bridges," Doctoral thesis, Southeast University, Dhaka, Bangladesh, 2015.

[12] X. S. Sun, "Experimental study on shear behavior of joints in precast segmental bridges," Master's thesis, Southeast University, Dhaka, Bangladesh, 2015.

[13] J. Muller, "Construction of long key bridge," *PCI Journal*, vol. 25, no. 6, pp. 97–111, 1980.

[14] J. Muller, "Twenty-five years of concrete segmental bridges—survey of behavior and maintenance costs," Company Report, Jean Muller International, San Diego, CA, USA, 1990.

[15] M. A. Issa and H. A. Abdalla, "Structural behavior of single key joints in precast concrete segmental bridges," *Journal of Bridge Engineering*, vol. 12, no. 3, pp. 315–324, 2007.

[16] F. M. Alkhairi, *On the Flexural Behavior of Concrete Beams Prestressed with Unbonded Internal and External Tendons*, University of Michigan, Ann Arbor, MI, USA, 1992.

[17] K. Koseki and J. E. Breen, *Exploratory Study of Shear Strength of Joints for Precast Segmental Bridges*, The University of Texas at Austin, Austin, TX, USA, 1983.

[18] J. Turmo, G. Ramos, and A. C. Aparicio, "Shear strength of dry joints of concrete panels with and without steel fibres: application to precast segmental bridges," *Engineering Structures*, vol. 28, no. 1, pp. 23–33, 2006.

[19] T. Wakasa, H. Otsuka, and W. Yabuki, "Experimental study of the shear strength of precast segmental beams with external prestressing," *Structural Concrete*, vol. 6, no. 2, pp. 63–80, 2005.

[20] F. Yan, C. Tian, W. Hao, J. Gao, and Y. Tan, "Experimental study on shear performance of joint surface between precast beam end and post-cast concrete," *Building Structure*, vol. 46, no. 10, pp. 74–79, 2016.

[21] L. J. Tao, P. Ding, C. Shi, X. W. Wu, S. Wu, and S. C. Li, "Shaking table test on seismic response characteristics of prefabricated subway station structure," *Tunnelling and Underground Space Technology*, vol. 91, 2019.